Temporally controlled ablation of PTEN in adult mouse prostate epithelium generates a model of invasive prostatic adenocarcinoma

Chandrahas Koumar Ratnacaram, Marius Teletin, Ming Jiang, Xiangjun Meng, Pierre Chambon*, and Daniel Metzger

Department of Functional Genomics, Institut de Génétique et de Biologie Moléculaire et Cellulaire, F-67400 Illkirch, France; Institut National de la Santé et de la Recherche Médicale, Unité 596, F-67400 Illkirch, France; Centre National de la Recherche Scientifique, Unité Mixte de Recherche 7104, F-67400 Illkirch, France; Université Louis Pasteur, F-67000 Strasbourg, France; and Collège de France, F-67400 Illkirch, France

Contributed by Pierre Chambon, December 20, 2007 (sent for review December 4, 2007)

Studies of prostate cancer pathogenesis and development of new therapies have been hampered by a lack of appropriate mouse models. We have generated PSA-Cre-ER^{T2} mice that express the tamoxifen-dependent Cre-ER^{T2} recombinase selectively in prostatic epithelium, thus allowing us to target floxed genes selectively in epithelial cells of fully differentiated prostate of adult mice and to modulate the number of genetically altered cells. Our present mouse model, in which prostate carcinogenesis is initiated through Cre-ER^{T2}-mediated somatic biallelic ablation of the tumor suppressor gene PTEN after puberty, closely mimics the course of human cancer formation. Indeed, mutant mice developed prostate epithelium hyperplasia within 4 weeks after PTEN ablation and prostatic intraepithelial neoplasia (PIN) in all lobes within 2–3 months, with the highest incidence in the dorsolateral lobe, which is considered to be the most similar to the peripheral zone of the human prostate, in which adenocarcinoma is preferentially localized. Eight to 10 months after PTEN ablation some PINs of the dorsolateral lobe had progressed to adenocarcinoma, but no distant metastases were found up to 20 months after PTEN ablation, indicating that progression to metastasis requires an additional mutation or mutations. Interestingly, monoallelic Cre-ER^{T2}-mediated PTEN ablation in epithelial cells of adult prostate also generated focal hyperplasia and PINs, but exclusively in the dorsolateral lobe, and in much lower number and after a longer latency. However, no progression to adenocarcinoma was observed. Because PTEN expression was undetectable in epithelial cells from these PINs, loss of PTEN function appears to act as a permissive event for uncontrolled cell proliferation.

Cre-ER^{T2} | prostate cancer | prostatic intraepithelial neoplasia | somatic mutagenesis

Prostate cancer, the most common cancer among North American and European men, affects one in nine men over 65 years of age. Its progression proceeds through a series of defined states, which include prostatic intraepithelial neoplasia (PIN) and prostate adenocarcinoma *in situ*, followed by locally invasive adenocarcinoma and eventually metastatic cancer. Because there is currently no effective cure for advanced stages of this disease, it is the third-leading cause of male cancer deaths (1, 2).

PTEN (phosphatase and tensin homolog deleted on chromosome 10), a tumor suppressor gene residing within 10q23, is frequently deleted in various advanced human cancers, and PTEN mutations have been identified in 10–15% of all prostate tumors and in up to 60% of advanced prostate cancers (refs. 3 and 4 and references therein). PTEN is a lipid phosphatase that dephosphorylates phosphoinositides at position 3 of the inositol ring. The membrane phosphoinositide and the second messager, phosphatidylinositol 3,4,5-trisphosphate [PI(3,4,5)P_3], have been identified as physiological substrates of PTEN. Growth factor-stimulated production of PI(3,4,5)P_3 results in activation of cell survival and proliferation mediated by phosphatidylinositol 3-kinase–protein kinase B/AKT signaling (5).

Various mouse lines aimed at exploring the molecular mechanisms underlying prostate carcinogenesis were generated over recent years by introducing targeted mutations selectively in prostatic epithelium (6, 7). Conditional PTEN floxed alleles were generated in the mouse, and PTEN was subsequently ablated in the prostate through breeding with transgenic mice expressing the Cre recombinase under the control of the mouse mammary tumor virus promoter [MMTV-Cre (8)], a modified probasin promoter [PB4-Cre (9–12)], or the prostate-specific antigen (PSA) promoter [PSA-Cre (13)]. Although these mouse model lines showed that the loss of PTEN was instrumental in prostate tumorigenesis, the occurrence and progression of the generated tumors did not closely mimic the spatiotemporal features exhibited by human prostatic tumors, and their latency, penetrance, and severity were different among the various transgenic lines. It was suggested that these variations could result from differences in the genetic background of the various model lines, as well as in time and/or efficiency of PTEN ablation in prostatic epithelial cells.

To control the cell specificity, the time of occurrence, and the cell extent of targeted somatic mutagenesis in the prostatic epithelium, we have generated PSA-Cre-ER^{T2} transgenic mice that express the tamoxifen (Tam)-dependent Cre-ER^{T2} recombinase (14) under the control of the human PSA promoter. We show that LoxP-flanked (floxed) PTEN L2 alleles are selectively ablated in prostatic epithelial cells by Tam administration to postpubertal PSA-Cre-ER^{T2}/PTEN$^{L2/L2}$ mice (PTEN$^{pe-/-}$ mice). Recombination occurred with the highest efficiency (in >35% of luminal epithelial cells) in the dorsolateral lobe, whose characteristics are the closest to human prostate (6), and with lower efficiencies in the ventral and anterior lobes. Moreover, by administrating Tam at lower doses, the number of targeted epithelial cells was reduced, thus offering the possibility to modulate the number of focal genetic lesions. All PTEN$^{pe-/-}$ mice developed prostate epithelium hyperplasia within 4 weeks after Tam administration and within 2–3 months developed PIN lesions in all lobes, with the highest incidence in the dorsolateral lobe. Moreover, 8–10 months after PTEN ablation some PINs located in the dorsolateral lobe had progressed to invasive

Author contributions: C.K.R., M.T., and M.J. contributed equally to this work; P.C. and D.M. contributed equally to this work; P.C. and D.M. designed research; C.K.R., M.T., M.J., and X.M. performed research; C.K.R., M.T., M.J., P.C., and D.M. analyzed data; and P.C. and D.M. wrote the paper.

The authors declare no conflict of interest.

*To whom correspondence should be addressed at: Institut de Génétique et de Biologie Moléculaire et Cellulaire, 1 Rue Laurent Fries, F-67400 Illkirch, France. E-mail: chambon@igbmc.u-strasbg.fr.

This article contains supporting information online at www.pnas.org/cgi/content/full/0712021105/DC1.

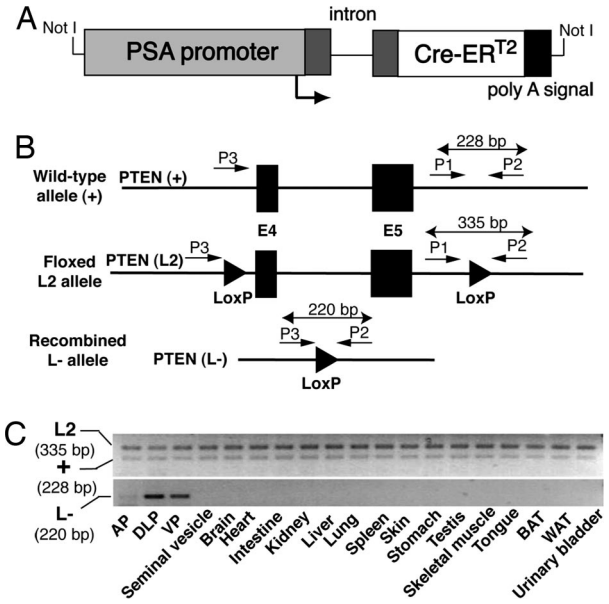

Fig. 1. Cre-ER^{T2}-mediated excision of floxed PTEN (exons 4 and 5) in PSA-Cre-ER^{T2} transgenic mice. (*A*) Schematic representation of the PSA-Cre-ER^{T2} transgene. The human PSA promoter is followed by rabbit β-globin noncoding exons (dark gray) interrupted by an intron, the Cre-ER^{T2} coding region, and by a SV40 poly(A) signal (black box). The transcription initiation site is marked by an arrow. (*B*) Schematic representation of wild-type (+), floxed (L2), and recombined (L−) PTEN alleles. Black boxes, arrowheads, and arrows indicate exons, LoxP sites, and PCR primers, respectively. (*C*) Characterization of Cre-mediated recombination in Tam-treated PSA-Cre-ER$^{T2(tg/0)}$/PTEN$^{L2/+}$ mice. Genomic DNA isolated at D12 from the indicated organs/cell types of a Tam-treated [from D1 to D5 (1.0 mg/day)] PSA-Cre-ER$^{T2(tg/0)}$/PTEN$^{L2/+}$ mouse was analyzed by semiquantitative PCR. The positions of the PTEN wild-type (228 bp), floxed (L2, 335 bp), and recombined (L−, 220 bp) DNA segments are indicated. The level of wild-type (+) allele PCR product indicates that a similar amount of genomic DNA was amplified from each tissue/cell type. BAT, brown adipose tissue; WAT, white adipose tissue.

adenocarcinoma. However, no distant metastases were found up to 20 months after PTEN ablation. In contrast, monoallelic Cre-mediated prostate-selective ablation of PTEN induced only few PIN lesions in dorsolateral prostate, and no progression to adenocarcinoma was observed.

Results

Generation of PSA-Cre-ER^{T2} Transgenic Mice for Selective Temporally Controlled Cre-Mediated Recombination in Prostatic Epithelium. To create temporally controlled targeted somatic mutations in the mouse prostatic epithelium, we generated transgenic mice expressing the Tam-dependent Cre-ER^{T2} recombinase under the control of the human PSA proximal promoter and androgen-dependent enhancer sequences (Fig. 1*A*). Of nine PSA-Cre-ER^{T2} transgenic founder mice, seven transmitted the PSA-Cre-ER^{T2} transgene through germ line (data not shown). To characterize Cre-ER^{T2}-mediated excision of LoxP-flanked (floxed) DNA, hemizygous transgenic mice from each of the seven PSA-Cre-ER$^{T2(tg/0)}$ lines were bred with heterozygote floxed PTEN$^{L2/+}$ mice (15) bearing a floxed PTEN allele, hereafter called PTEN L2 allele (Fig. 1*B*). Tam administration [1 mg/day from day (D)1 to D5] to 8-week-old PSA-Cre-ER$^{T2(tg/0)}$/PTEN$^{L2/+}$ bigenic mice induced selective Cre-mediated DNA excision in the prostate from mice derived from one of the seven lines (Fig. 1*C*), called hereafter PSA-Cre-ER^{T2}. No Cre-mediated recombination was observed in any organ of vehicle-treated mice from this line (data not shown). Note that excision of the floxed DNA was more efficient in the dorsolateral prostate (DLP) than in the ventral prostate (VP) and that little recombination was detected in the anterior prostate (AP) (see also below).

To further characterize Tam-induced recombinase activity in PSA-Cre-ER^{T2} mice, these mice were bred with RosaR26R reporter mice that express β-galactosidase after Cre-mediated recombination (16). Bigenic PSA-Cre-ER^{T2}/RosaR26R mice were Tam-treated (D1–D5) at 8 weeks, and β-galactosidase expression was analyzed at D14 by immunohistrochemistry using an antibody directed against *Escherichia coli* β-galactosidase, because prostate exhibits high endogenous β-galactosidase activity. Approximately 30–40% of epithelial cells were immunostained in DLP and VP, and <10% were immunostained in AP (data not shown). Stromal cells did not express *E. coli* β-galactosidase after Tam treatment, and no *E. coli* β-galactosidase expression was observed in the prostatic lobes from oil-treated PSA-Cre-ER^{T2}/RosaR26R mice (data not shown). Taken together, these data show that Cre-mediated recombination was selectively induced in prostatic epithelial cells of PSA-Cre-ER^{T2} mice upon Tam treatment. However, the efficiency of Cre-mediated excision of floxed DNA was variable depending on the nature of the floxed target gene. For example, ≈75–80% of floxed RXRα L2 alleles were recombined in DLP and VP, and >65% were recombined in the AP, after Tam treatment of PSA-Cre-ER$^{T2(tg/0)}$/RXR$\alpha^{L2/L2}$ mice [supporting information (SI) Fig. 5]. Note that all quantitative PCR values underscore the efficiency of DNA recombination in epithelial cells, because genomic DNA was extracted not only from these cells, but also from stromal cells in which the Cre-ER^{T2} recombinase is not expressed.

Selective Cre-ER^{T2}-Mediated Biallelic Ablation of PTEN in Prostatic Epithelial Cells of Adult Mice Leads to PIN That Progresses to Adenocarcinoma. To selectively ablate PTEN in the prostatic epithelium of adult mice, 8-week-old PSA-Cre-ER$^{T2(tg/0)}$/PTEN$^{L2/L2}$ animals bearing two PTEN L2 alleles were Tam-treated (1 mg/day) from D1 to D5, thus generating prostatic epithelium-specific PTEN L−/L− mice, called hereafter PTEN$^{pe-/-}$ mice. Quantitative PCR of DNA extracted at D12 showed that 35%, 31%, and 8% of the PTEN L2 alleles were recombined in DLP, VP, and AP, respectively (SI Fig. 6). Immunohistochemical analyses performed at D26 showed that PTEN protein was readily detected in the cytoplasm of all AP, DLP, and VP epithelial cells of Tam-treated control (CT) mice (PTEN$^{L2/L2}$ mice that lack the transgene) (Fig. 2 *Aa–Ai* and data not shown), in agreement with previous reports (9). In PTEN$^{pe-/-}$ mice, PTEN immunostaining was lost in a patchy manner (Fig. 2 *Ba–Bi* and data not shown). In DLP, loss of PTEN was observed in ≈30–40% of epithelial cells in most of the ducts (Fig. 2 *Bd–Bf* and data not shown). Because down-regulation of PTEN is known to activate the AKT serine:threonine kinase (17), the plasma membrane localization of phosphorylated AKT (P-AKT) can serve as a reliable indicator for PTEN loss. As expected, the loss of PTEN protein in DLP epithelial cells resulted in phosphorylation of AKT that accumulates at the plasma membrane (Fig. 2 *Bm–Bo*). PTEN loss was observed in ≈20% of epithelial cells of only 70% of VP ducts (Fig. 2 *Bg–Bi* and *Bp–Br* and data not shown) and in <5% of epithelial cells of ≈30% AP ducts (Fig. 2 *Ba–Bc* and *Bj–Bl* and data not shown). In contrast, PTEN immunostaining remained positive in the stromal compartment, and no P-AKT immunostaining was observed in these cells (data not shown), thus indicating the selective ablation of PTEN in prostatic epithelial cells. Moreover, because no PTEN loss and no P-AKT immunoreactivity was seen in prostate of oil (vehicle)-treated PSA-Cre-ER$^{T2(tg/0)}$/PTEN$^{L2/L2}$ mice (data not shown), PTEN ablation was strictly Tam-dependent. Note that Tam administration at 0.25 mg/day for 5 days to PSA-Cre-ER$^{T2(tg/0)}$/PTEN$^{L2/L2}$ mice, instead of 1 mg/day, resulted at D12 in PTEN

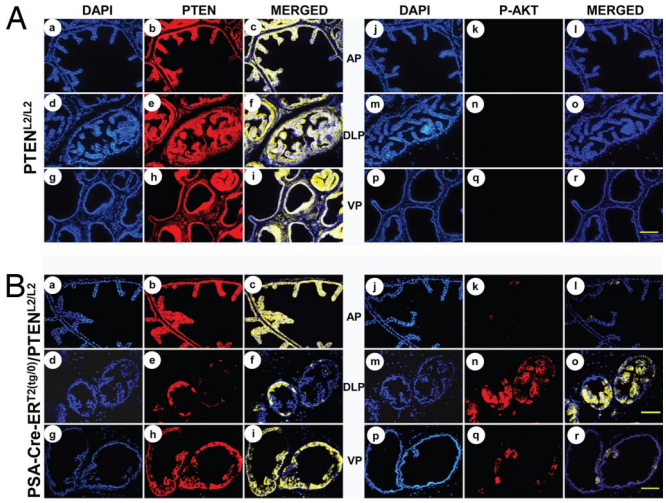

Fig. 2. Cre-mediated PTEN ablation in prostatic lobes of PSA-Cre-ER$^{T2(tg/0)}$/PTEN$^{L2/L2}$ mice. (*A* and *B*) Immunohistochemical detection of PTEN (*a–i*) and P-AKT (*j–r*) (adjacent sections) in AP (*a–c* and *j–l*), DLP (*d–f* and *m–o*), and VP (*g–i* and *p–r*) lobes of control PTEN$^{L2/L2}$ (*A*) and PSA-Cre-ER$^{T2(tg/0)}$/PTEN$^{L2/L2}$ (*B*) mice 3 weeks after Tam administration. *a*, *d*, *g*, *j*, *m*, and *p* show DAPI staining (blue) of nuclei; *b*, *e*, and *h* show PTEN immunodetection (red); and *k*, *n*, and *q* show P-AKT immunodetection (red). In *c*, *f*, *i*, *l*, *o*, and *r*, DAPI and immunostaining (yellow false color) are merged. (Scale bars: *A*, *Ba–Bc*, *Bg–Bl*, and *Bp–Br*, 200 μm; *Bd–Bf* and *Bm–Bo*, 150 μm.)

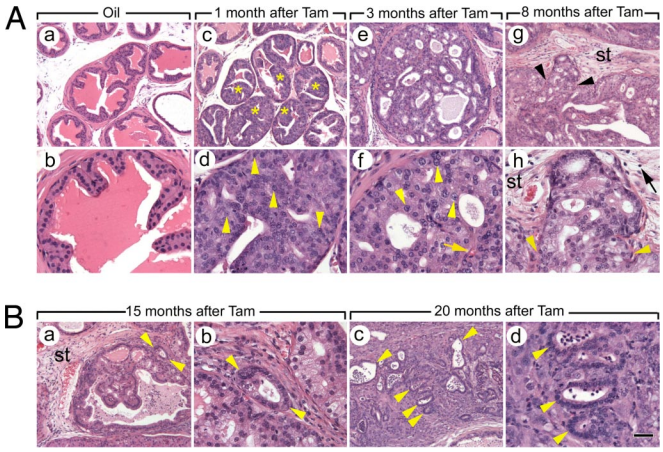

Fig. 3. Histological analysis of DLP lobes from PSA-Cre-ER$^{T2(tg/0)}$/PTEN$^{L2/L2}$ mice from 1 to 20 months after treatment with Tam at the age of 8 weeks. Shown is hematoxylin/eosin-stained DLP from PSA-Cre-ER^{T2}/PTEN$^{L2/L2}$ mice 1 month after oil administration (control) (*Aa* and *Ab*) (similar results were obtained 20 months after oil treatment and in PTEN$^{L2/L2}$ mice treated with Tam), as well as 1 (*Ac* and *Ad*), 3 (*Ae* and *Af*), and 8 (*Ag* and *Ah*) months after Tam treatment, and 15 (*Ba* and *Bb*) and 20 (*Bc* and *Bd*) months after Tam treatment. A well differentiated single layer of prostate epithelium is seem in *Aa* (low magnification) and *Ab* (high magnification). Hyperplasia and PIN lesions are indicated by yellow asterisks in *Ac* (low magnification). Yellow arrowheads in *Ad* (high magnification) point to atypical epithelial cells with prominent nucleoli. Massive epithelial cell hyperplasia and PIN lesions in enlarged prostate glands with smooth glandular profile are seen in *Ae* (low magnification). Atypical epithelial cells displaying abundant pale cytoplasm and nuclear pleiomorphism with prominent nucleoli are pointed by yellow arrowheads, and a small intraepithelial blood vessel is indicated by a yellow arrow in *Af* (higher magnification). Epithelial cells of a PIN filling almost entirely the lumen of the duct are shown in *Ag* (low magnification). Arrowheads in *Ag* and *Ah* (high magnification) indicate epithelial cells bulging into the adjacent stroma (st). Note that atypical cells are poorly oriented, presenting abundant pale cytoplasm with nuclear pleiomorphism and hyperchromasia. A black arrow in *Ah* points to inflammatory cells. Arrowheads in *Ba* point to microinvasive carcinoma in association with a PIN-containing gland. Higher magnification in *Bb* shows extension of a small malignant gland (arrowheads) into the adjacent thickened stroma. Invasive adenocarcinoma extending into the stroma is shown in *Bc* (low magnification) and *Bd* (high magnification). Note the presence of multiple malignant glands (arrowheads) with cells presenting nuclear pleiomorphism and hyperchromasia. st, stroma. (Scale bars: *Aa*, *Ac*, *Ae*, *Ag*, *Ba*, and *Bc*, 100 μm; *Ab*, *Ad*, *Af*, *Ah*, *Bb*, and *Bd*, 30 μm.)

ablation in a lower number of DLP epithelial cells, and almost no PTEN loss was observed in the other lobes (SI Fig. 7 and data not shown).

To determine the effect of PTEN ablation in epithelial cells of the mature prostate, we examined control and PTEN$^{pe-/-}$ mutant mice from 2 weeks to 20 months after Tam treatment. Up to 20 months after vehicle (oil) treatment, the morphology of the prostatic epithelium and stroma of PSA-Cre-ER$^{T2(tg/0)}$/PTEN$^{L2/L2}$ was similar to that of aged-matched wild-type mice (Fig. 3 *Aa* and *Ab* and data not shown), thus demonstrating that the presence of the PSA-Cre-ER^{T2} transgene and PTEN L2 alleles did not affect prostate development and did not induce any pathological changes on their own in adult mouse prostate. Similarly, up to 20 months after Tam treatment the prostates of PTEN$^{L2/L2}$ mice did not reveal any histological abnormalities, compared with aged-matched WT mice (data not shown).

In contrast, all PTEN$^{pe-/-}$ mice developed focal hyperplasia and PIN (18) between 2 and 4 weeks after Tam treatment (Table 1, Fig. 3 *Ac* and *Ad*, and data not shown). Recognizable features of PIN included proliferation of large atypical cells within preexisting prostatic ducts with enlarged nuclei, hyperchromasia, and prominent nucleoli. The DLP displayed the highest number (≈25–50%) of affected glands (Fig. 3*Ac*), whereas in the AP <10% of the ducts exhibited hyperplasia/PIN (data not shown), and in the VP <25% of the ducts displayed PINs (data not shown).

By 3 months after Tam treatment, PIN lesions were present in almost all of the ducts of DLP and VP and in only ≈25% of the ducts from AP with ≈10% of epithelial cells involved. Even though the DLP and VP showed a massive distension of all prostatic ducts, their profile remained smooth. Approximately 90% of the ducts from DLP were filled with cells with increased nuclear atypia in a tufting and cribriform growth pattern (Fig. 3 *Ae* and *Af*). Mitotic figures and intraepithelial blood vessels were also observed (Fig. 3*Af* and data not shown). In VP and AP fewer glands were affected and PINs were less severe (data not shown). At this stage, most of the epithelial cells of DLP were PTEN-deficient and expressed P-AKT, indicating that PTEN-deficient cells actively proliferated, whereas the number of PTEN-deficient epithelial cells was not >40–50% in VP (SI Fig. 8).

By 8 months after Tam treatment, PIN lesions extended into nearly all ducts of the DLP of all mice analyzed (Fig. 3*Ag*, Table 1, and data not shown). Epithelial cells were poorly oriented with increased nuclear hyperchromasia and pleiomorphism. The contour of the glands became distorted and bulged into the adjacent stroma (Fig. 3 *Ag* and *Ah*). Host response was present with inflammatory cells (Fig. 3*Ah*). Similar defects were seen in VP and AP but in only ≈70% and 50% of their ducts, respectively.

Eight to 14 months after Tam treatment, the prostates of all PTEN$^{pe-/-}$ mice were massively enlarged (data not shown), and their mass reached up to 4.7 g, corresponding to a 20- to 40-fold increase. Histological analysis revealed that in DLP few PIN lesions progressed to microinvasive and invasive adenocarcinomas in ≈60% of the mice as early as 8–10 months after Tam treatment, and in all of them 10–16 months after Tam treatment (Table 1). Interestingly, small malignant glands were invading the surrounding desmoplastic stroma (Fig. 3 *Ba* and *Bb*).

Cytokeratin K14 immunohistochemical staining showed that basal cells of PIN in DLP from PTEN$^{pe-/-}$ mice 4 months after Tam administration were increased in number and size compared with control prostate (SI Fig. 9*b* and data not shown).

Table 1. Morphologic alterations in DLP lobes of mice in which one or two floxed PTEN alleles were specifically ablated at the age of 8 weeks through Tam activation of the conditional Cre-ER^{T2} recombinase selectively expressed from the PSA-Cre-ER^{T2} transgene in prostatic epithelium

	Time lapse after Tam treatment				
Mouse genotype	Up to 1 month	2–3 months	4–6 months	8–10 months	14–16 months
Control*	4 of 4 normal	5 of 5 normal	5 of 5 normal	4 of 4 normal	3 of 3 normal
PTEN$^{pe-/+}$	ND	ND	1 of 5 focal hyperplasia, PIN	5 of 5 focal hyperplasia, PIN	3 of 3 focal hyperplasia, PIN
PTEN$^{pe-/-}$	3 of 3 focal hyperplasia, PIN	5 of 5 hyperplasia, PIN	4 of 4 hyperplasia, PIN	5 of 5 hyperplasia, PIN, 1 of 5 focal microinvasion, 2 of 5 invasive adenocarcinoma	3 of 3 hyperplasia, PIN, 3 of 3 invasive adenocarcinoma

ND, not determined.
*PTEN$^{L2/L2}$ mice treated with Tam or PSA-Cre-ER$^{T2(tg/0)}$/PTEN$^{L2/L2}$ mice treated with oil.

Moreover, basal cells vanished in malignant epithelial cells of invasive cancer (SI Fig. 9*c*). Androgen receptor immunostaining was strong in PIN lesions and remained positive but more diffuse in invasive cancer (SI Fig. 9 *e* and *f*, respectively). Finally, luminal cells in PIN and invasive tumors displayed robust immunostaining for cytokeratin K8, confirming the epithelial origin of these lesions (SI Fig. 9 *h* and *i*, respectively).

More advanced adenocarcinoma was observed in DLP 20 months after PTEN ablation, as multiple malignant glands with poorly differentiated cells extended into the stroma (Fig. 3 *Bc* and *Bd*). However, macroscopic examination of the organs from all analyzed PTEN$^{pe-/-}$ mice and analysis of caudal para-aortic lymph node serial sections from six mice between 8 and 20 months after Tam treatment did not reveal any metastasis. Note that no adenocarcinoma could be found in VP and AP of PTEN$^{pe-/-}$ mice 8–20 months after PTEN ablation.

Selective Cre-Mediated Ablation of One PTEN Allele in Prostatic Epithelial Cells of Adult Mice Leads to PIN Within 4–8 Months. To determine the effect of Cre-mediated deletion of one PTEN allele in adult prostatic epithelium, PSA-Cre-ER$^{T2(tg/0)}$/PTEN$^{L2/+}$ (PTEN$^{pe-/+}$) mice were analyzed 4–20 months after PTEN ablation. Interestingly, at 4 months one of five PTEN$^{pe-/+}$ mice displayed lesions of focal hyperplasia and PIN in ≈10–20% of the DLP ducts, and after 8 months all PTEN$^{pe-/+}$ mice exhibited PINs (Fig. 4*A*, Table 1, and data not shown). However, no adenocarcinoma was seen in these mice up to 20 months after Tam treatment. Moreover, no histological defects were seen in VP and AP of PTEN$^{pe-/+}$ mice. Interestingly, immunohistochemical analysis showed a loss of PTEN expression and concomitant P-AKT up-regulation that was restricted to the focal PIN lesions in PTEN$^{pe-/+}$ mice (Fig. 4*B* and data not shown), showing that the second PTEN allele was silenced in these PIN lesions.

Discussion

Studies of the molecular mechanisms underlying human prostate carcinogenesis, as well as the development and validation of new therapies, have been hampered by a lack of mouse models that mimic the genetic alterations and clinical course of prostate cancer in humans. Several transgenic mouse lines that express Cre recombinase selectively in the prostatic epithelium have been recently established to conditionally target floxed genes in prostate (13, 19–21). However, even though the use of these lines has shed light into prostate carcinogenesis, the lack of temporal control of Cre recombinase expression or activity remained a major drawback, as ablation of target genes occurred before puberty completion, and therefore before prostate was fully differentiated. Moreover, because in these mouse lines the Cre recombinase is constitutively expressed in prostatic epithelial cells, the number of genetically altered cells cannot be modulated. Thus, these mouse lines do not allow us to generate, in adult mouse prostatic epithelial cells, focal targeted mutations whose number and initiation timing could be modulated to mimic the human prostate carcinogenetic process.

To circumvent these problems, we generated PSA-Cre-ER^{T2} transgenic mice that express the Tam-dependent Cre-ER^{T2} recombinase under the control of the androgen-dependent human PSA promoter that is selectively active in prostatic epithelial cells throughout postpubertal mouse life. Whereas no Cre recombinase activity was observed in PSA-Cre-ER^{T2} adult mice in the absence of Tam treatment, Tam administration (1 mg/day for 5 days) induced Cre-mediated recombination selectively in prostatic epithelial cells of all lobes, thus allowing us to generate temporally controlled targeted somatic mutations selectively in the prostatic epithelium. Gene targeting was most efficient in the dorsolateral lobe, which is considered to be the most similar to the peripheral zone of human prostate, in which

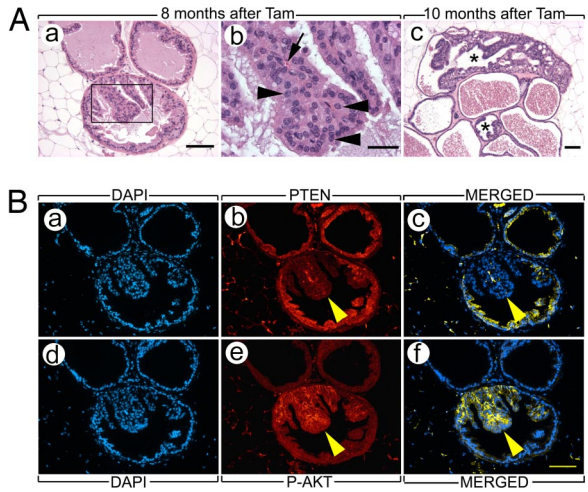

Fig. 4. Histological analysis of DLP lobe from PTEN$^{pe-/+}$ mice 8 and 10 months after Tam treatment. (*A*) Hematoxylin/eosin-stained DLP sections from PTEN$^{pe-/+}$ mice 8 (*Aa* and *Ab*) and 10 (*Ac*) months after Tam treatment. (*Aa*) Section with a gland containing a PIN (boxed region). (*Ab*) Higher magnification of the PIN shown in *Aa*. Note the presence of enlarged atypical nuclei (arrowhead in *Ab*) and intraepithelial blood vessel (arrow in *Ab*). (*Ac*) Section with two of eight ducts containing PINs (asterisk). (Scale bars: *Aa* and *Ac*, 100 μm; *Ab*, 30 μm.) (*B*) Immunohistochemical detection of PTEN (*Ba–Bc*) and P-AKT (*Bd–Bf*) (sections adjacent to *Aa*). (*Ba* and *Bd*) DAPI staining (blue) of nuclei. (*Bb* and *Be*) PTEN and P-AKT immunodetection, respectively. (*Bc* and *Bf*) DAPI and immunostaining (yellow false color) are merged. Arrowheads point to the PIN lesion. (Scale bar: 100 μm.)

adenocarcinoma is preferentially localized (6). Moreover, the number of epithelial cells that undergo Cre-mediated recombination could be decreased by lowering the dose of Tam administered, thus offering the possibility to generate genetic alterations that resemble those found in human cancer.

Our present mouse model, in which prostate carcinogenesis can be initiated through Cre-ER^{T2}-mediated biallelic ablation of the PTEN suppressor gene at any chosen time during postpubertal life, closely mimics the course of human cancer formation (see Table 1): focal hyperplasia of epithelial cells occurs within 4 weeks after PTEN ablation, and by 2–3 months PINs have grown in all three lobes of all mutant mice with a reproducible kinetics, albeit with a higher density in the dorsolateral lobe. Interestingly, PINs then progress by 8–10 months to invasive adenocarcinoma in the dorsolateral lobe exclusively. However, no further progression to metastatic tumors could be detected in older mice (up to 20 months after PTEN ablation), which indicates that mutation in an additional gene or genes is likely to be required to generate metastasis.

Our present prostate cancer model exhibits both similarities and differences with previously established mouse models in which PTEN was selectively ablated in the prostatic epithelium by using transgenic mice expressing the Cre recombinase under the control of a composite probasin promoter [PB-Cre4 (9, 11)] or the PSA promoter [PSA-Cre (13)]. PTEN ablation generated prostatic epithelial cell hyperplasia and PINs in these models, but the kinetics and extent of tumor progression were different in the various models. Invasive adenocarcinoma was generated within 2 months in the studies of both Trotman *et al.* (11) and Wang *et al.* (9), but in the latter study metastases were observed after 3 months in ≈50% of mutant mice. In contrast, using transgenic PSA-Cre mice, invasive carcinoma was observed only in mutant mice >7 months old, and lymph node metastasis was found in only one aged mutant mouse (13), indicating that metastasis was a rare event. Because the mutant lines used in these studies were on different mixed genetic backgrounds, and knowing that the genetic background could modify the tumorigenesis caused by PTEN mutation (22), some of these differences (e.g., metastasis) could reflect the existence of modifier genes. In addition, the developmental stage at which PTEN ablation takes place, and its extent in the prostatic epithelium, both of which depend on the activity and cell specificity of the composite probasin and PSA promoters, could also affect tumorigenesis.

Interestingly, monoallelic Cre-ER^{T2}-mediated PTEN ablation in epithelial cells of adult prostate (PTEN$^{pe-/+}$ mice) also generated focal hyperplasia and PINs, but exclusively in the dorsolateral lobe and in much lower number and after a longer latency than in the case of biallelic PTEN-ablated (PTEN$^{pe-/-}$) mice: PINs were observed with a full penetrance in the dorsolateral lobe of PTEN$^{pe-/+}$ mice only 8 months after Tam treatment, whereas no PINs could be observed in the other lobes, even in older mice. Strickingly, immunohistochemical analyses showed that epithelial cells of PINs from PTEN$^{pe-/+}$ mice did not express PTEN, in contrast to other prostatic epithelial cells, indicating that PTEN loss of function represents an initial event permissive for uncontrolled cell proliferation. That no adenocarcinoma was observed in up to 22-month-old PTEN$^{pe-/+}$ mice indicates that the average latency period to progress from PINs to carcinoma is at least 12 months. Because the pathological changes observed in PTEN$^{pe-/+}$ mice are more severe than those induced by PSA-Cre-mediated monoallelic PTEN ablation in the prostatic epithelium (13), where only focal dysplasia was observed in only 20% of 10- to 14-month-old mice, and are quite similar to those observed in hemizygote PTEN$^{+/-}$ mice (23–25), it is unlikely that the timing of PTEN ablation, and the number and localization of targeted prostatic epithelial cells, or the loss of function of one PTEN allele in prostatic stromal cells or in other nonepithelial cells, have major effects on prostate cancer initiation.

Taken together, the present data show that our murine prostate cancer model recapitulates with defined kinetics the disease progression seen in humans, with the exception of metastasis. Compared with previous murine models of prostate carcinogenesis, our model offers major improvements that are intrinsic to our targeted spatiotemporally controlled Cre-ER^{T2}-mediated somatic mutagenesis (26): first, it allows us to introduce, selectively in prostatic epithelial cells, a somatic mutation targeted to any selected floxed gene at any time during the postpubertal life of the mouse; second, it allows us to modulate the number of cells in which the mutation is introduced. Our model should be particularly valuable both for exploring the molecular mechanisms underlying prostate cancer and its progression and for the development and validation of preventive and therapeutic approaches in preclinical settings. It should also provide a unique tool in searches for genes whose genetic alterations may lead to, or prevent, metastasis, particularly in bone. Moreover, the PSA-Cre-ER^{T2} transgenic mouse should be very helpful for generating humanized mouse models of human prostate cancer through combinations of germ-line and temporally controlled cell-specific mutations.

Materials and Methods

Mice. To generate PSA-Cre-ER^{T2} transgenic mouse lines, a 6.0-kb PCR-amplified DNA segment containing the proximal promoter and enhancer of human PSA gene (27, 28) was cloned into the SalI site of pGS-Cre-ER^{T2} (29), yielding pPSA-Cre-ER^{T2}. The 9.8-kb NotI-restricted PSA-Cre-ER^{T2} transgene (Fig. 1*A*) was isolated, purified, and microinjected into fertilized eggs as described (30). Floxed homozygous PTEN mice (hereafter called PTEN$^{L2/L2}$ mice) and RosaR26R Cre reporter mice have been described (15, 16). PSA-Cre-ER^{T2} and floxed PTEN mice were genotyped as described (15, 30). PSA-Cre-ER$^{T2(tg/0)}$/PTEN$^{L2/L2}$ and PTEN$^{L2/L2}$ control littermates were on a 75% C57BL6, 15% 129 SV, and 10% FVBN mixed background. Tam administration [daily injection for 5 days (D1–D5)] to 8-week-old mice was performed as described (31). Breeding and maintenance of mice were performed under institutional guidelines.

PCR Analysis. Genomic DNA isolated from various mouse organs was amplified by PCR as described (31). Sense primer P1 (5′-CTCCTCTACTCCATTCTTCCC-3′) and antisense primer P2 (5′-ACTCCCACCAATGAACAAAC-3′) were used to amplify the 228-bp PTEN WT and 335-bp PTEN L2 DNA segments, and sense primer P3 (5′-GGTTTAAGATTGTATGTGATCATCT-3′) and antisense primer P2 were used to amplify the 220-bp PTEN L− DNA segment (Fig. 1).

Histological Analysis. After fixation in buffered formaldehyde for 24 h, prostate samples were embedded in paraffin, serially sectioned at 5 μm, and stained with hematoxylin and eosin. For histopathological analyses, paraffin sections were stained with hematoxylin and eosin. For immunohistochemical staining, paraffin sections were placed on SuperFrost plus charged glass slides (Menzel-Glaser). Microwave pretreatment [740 W for 7.30 min in 0.01 M citric acid buffer (pH 6.0)] and cooling at room temperature for 30 min were applied to retrieve antigens. Slides were washed in PBS with Tween 0.05% (PBST, four times for 5 min) followed by PBS wash (once for 5 min) (32) and incubated in 5% normal goat serum (Vector Laboratories) for 1 h and with primary antibody (diluted 1/50) [rabbit polyclonal anti-PTEN (catalog no. 9552; Cell Signaling Technology), and rabbit polyclonal anti-pAKT (Ser-473) (catalog no. 9571; Cell Signaling Technology)] overnight at 4°C. Thereafter slides were washed in PBST (four times for 5 min), incubated with CY3 AffiniPure goat anti-rabbit IgG (H+L) antibodies (Jackson ImmunoResearch) for 1 h at room temperature, washed in PBST (four times for 5 min), and mounted with Vectashield mounting medium (Vector Laboratories) containing DAPI (Invitrogen).

Other Methods. Quantification of PTEN and RXRα alleles, and immunodetection of K14, K8, and AR, are described in *SI Text*.

ACKNOWLEDGMENTS. We thank P. Soriano for RosaR26R mice; T. Mak (Campbell Family Institute for Breast Cancer Research, Toronto) and A. Suzuki (Akita University School of Medicine, Akita, Japan) for floxed PTEN mice; Manuel Mark (Fred Hutchinson Cancer Research Center, Seattle) for helpful discus-

sions; and Mirella Nastasi, Jean-Marc Bornert, Jean-François Kleinmann, Olivia Wendling, Fabrice Auge, and the staff of the transgenic and animal facilities for excellent technical assistance. This work was supported by funds from the Centre National de la Recherche Scientifique, the Institut National de la Santé et de la Recherche Médicale, the Collège de France, the Ministère de l'Enseignement Supérieur et de la Recherche, and the Association pour la Recherche sur le Cancer. C.K.R. was supported by fellowships from the Fondation pour la Recherche Médicale and the Association pour la Recherche à l'Institut de Génétique et de Biologie Moléculaire et Cellulaire. M.T. was supported by European Community Project Eumorphia PLRT-CT-2001-00930, and M.J. and X.M. were supported by fellowships from the Association pour le Développement de la Recherche Génétique Moléculaire.

1. Parkin DM, Bray F, Ferlay J, Pisani P (2005) Global cancer statistics, 2002. *CA Cancer J Clin* 55:74–108.
2. Abate-Shen C, Shen MM (2000) Molecular genetics of prostate cancer. *Genes Dev* 14:2410–2434.
3. Li J, *et al*. (1997) PTEN, a putative protein tyrosine phosphatase gene mutated in human brain, breast, and prostate cancer. *Science* 275:1943–1947.
4. Ali IU, Schriml LM, Dean M (1999) Mutational spectra of PTEN/MMAC1 gene: A tumor suppressor with lipid phosphatase activity. *J Natl Cancer Inst* 91:1922–1932.
5. Chow LM, Baker SJ (2006) PTEN function in normal and neoplastic growth. *Cancer Lett* 241:184–196.
6. Roy-Burman P, Wu H, Powell WC, Hagenkord J, Cohen MB (2004) Genetically defined mouse models that mimic natural aspects of human prostate cancer development. *Endocr Relat Cancer* 11:225–254.
7. Abate-Shen C, Shen MM (2002) Mouse models of prostate carcinogenesis. *Trends Genet* 18:S1–S5.
8. Backman SA, *et al*. (2004) Early onset of neoplasia in the prostate and skin of mice with tissue-specific deletion of Pten. *Proc Natl Acad Sci USA* 101:1725–1730.
9. Wang S, *et al*. (2003) Prostate-specific deletion of the murine Pten tumor suppressor gene leads to metastatic prostate cancer. *Cancer Cell* 4:209–221.
10. Wang S, *et al*. (2006) Pten deletion leads to the expansion of a prostatic stem/progenitor cell subpopulation and tumor initiation. *Proc Natl Acad Sci USA* 103:1480–1485.
11. Trotman LC, *et al*. (2003) Pten dose dictates cancer progression in the prostate. *PLoS Biol* 1:E59.
12. Chen Z, *et al*. (2005) Crucial role of p53-dependent cellular senescence in suppression of Pten-deficient tumorigenesis. *Nature* 436:725–730.
13. Ma X, *et al*. (2005) Targeted biallelic inactivation of Pten in the mouse prostate leads to prostate cancer accompanied by increased epithelial cell proliferation but not by reduced apoptosis. *Cancer Res* 65:5730–5739.
14. Feil R, Wagner J, Metzger D, Chambon P (1997) Regulation of Cre recombinase activity by mutated estrogen receptor ligand-binding domains. *Biochem Biophys Res Commun* 237:752–757.
15. Suzuki A, *et al*. (2001) T cell-specific loss of Pten leads to defects in central and peripheral tolerance. *Immunity* 14:523–534.
16. Soriano P (1999) Generalized lacZ expression with the ROSA26 Cre reporter strain. *Nat Genet* 21:70–71.
17. Stambolic V, *et al*. (1998) Negative regulation of PKB/Akt-dependent cell survival by the tumor suppressor PTEN. *Cell* 95:29–39.
18. Shappell SB, *et al*. (2004) Prostate pathology of genetically engineered mice: Definitions and classification. The consensus report from the Bar Harbor meeting of the Mouse Models of Human Cancer Consortium Prostate Pathology Committee. *Cancer Res* 64:2270–2305.
19. Maddison LA, Nahm H, DeMayo F, Greenberg NM (2000) Prostate specific expression of Cre recombinase in transgenic mice. *Genesis* 26:154–156.
20. Wu X, *et al*. (2001) Generation of a prostate epithelial cell-specific Cre transgenic mouse model for tissue-specific gene ablation. *Mech Dev* 101:61–69.
21. Jin C, McKeehan K, Wang F (2003) Transgenic mouse with high Cre recombinase activity in all prostate lobes, seminal vesicle, and ductus deferens. *Prostate* 57:160–164.
22. Freeman D, *et al*. (2006) Genetic background controls tumor development in PTEN-deficient mice. *Cancer Res* 66:6492–6496.
23. Di Cristofano A, Pesce B, Cordon-Cardo C, Pandolfi PP (1998) Pten is essential for embryonic development and tumour suppression. *Nat Genet* 19:348–355.
24. Stambolic V, *et al*. (2000) High incidence of breast and endometrial neoplasia resembling human Cowden syndrome in pten+/− mice. *Cancer Res* 60:3605–3611.
25. Podsypanina K, *et al*. (1999) Mutation of Pten/Mmac1 in mice causes neoplasia in multiple organ systems. *Proc Natl Acad Sci USA* 96:1563–1568.
26. Metzger D, *et al*. (2003) Targeted conditional somatic mutagenesis in the mouse: Temporally-controlled knockout of retinoid receptors in epidermal keratinocytes. *Methods Enzymol* 364:379–408.
27. Cleutjens KB, *et al*. (1997) A 6-kb promoter fragment mimics in transgenic mice the prostate-specific and androgen-regulated expression of the endogenous prostate-specific antigen gene in humans. *Mol Endocrinol* 11:1256–1265.
28. Riegman PH, Vlietstra RJ, van der Korput JA, Brinkmann AO, Trapman J (1991) The promoter of the prostate-specific antigen gene contains a functional androgen responsive element. *Mol Endocrinol* 5:1921–1930.
29. Indra AK, *et al*. (1999) Temporally-controlled site-specific mutagenesis in the basal layer of the epidermis: Comparison of the recombinase activity of the tamoxifen-inducible Cre-ER(T) and Cre-ER(T2) recombinases. *Nucleic Acids Res* 27:4324–4327.
30. Feil R, *et al*. (1996) Ligand-activated site-specific recombination in mice. *Proc Natl Acad Sci USA* 93:10887–10890.
31. Metzger D, Li M, Chambon P (2005) Targeted somatic mutagenesis in the mouse epidermis. *Methods Mol Biol* 289:329–340.
32. Chapellier B, *et al*. (2002) Physiological and retinoid-induced proliferations of epidermis basal keratinocytes are differently controlled. *EMBO J* 21:3402–3413.